SAND2018-11864C

Techniques for Nonlinear Identification and Maximizing Modal Response

D. Roettgen, B. Pacini, R. Mayes

Structural Dynamics Department
Sandia National Laboratories*
P. O. Box 5800 – MS0557
Albuquerque, NM 87185

1. Abstract

Recent research has shown that weakly nonlinear structures can be modeled as a combination of nonlinear pseudo-modal models. These modal models consist of a linear spring, mass, and damper with the addition of a nonlinear element often identified using a restoring force surface technique. This approach is limited by force level achieved when exciting the system for identification. Extrapolation leads to poor results when predicting the nonlinear response; thus, there is a need to maximize the modal amplitude excited in these weakly nonlinear structures. Previous works have compared hammer testing to shaker testing using windowed sinusoidal input forces. This appeared to be a promising technique to increasing the excited modal amplitude. In this work the windowed sinusoidal technique is further investigated to understand how window parameters (such as window width) can be optimized to maximize the modal amplitude obtained during the identification process.

Keywords – Nonlinear system identification, experimental techniques, structural dynamics, modal analysis, nonlinear testing methods

*Sandia National Laboratories is a multimission laboratory managed and operated by National Technology and Engineering Solutions of Sandia, LLC., a wholly owned subsidiary of Honeywell International, Inc., for the U.S. Department of Energy's National Nuclear Security Administration under contract DE-NA-0003525.

2. Introduction

Many industries design and manufacture mechanical structures with bolted joints. The frictional interfaces that occur due to these joints often introduce nonlinearity into an otherwise linear system. Two main approaches exist to account for these nonlinearities: local physical models and pseudo-modal modeling [1, 2, 3]. Local physical modeling attempts to capture the physics happening at each local joint. While physically insightful, this method can be computationally expensive, and the constitutive models require expensive calibration for every structural joint. Nonlinear pseudo-modal modeling is computationally inexpensive, and nonlinear parameters can be identified from a quick experiment focused on each nonlinear mode. In this work, a weakly nonlinear system is studied which exhibited small shifts in frequency with large changes in damping. In previous works [4, 5] pseudo-modal modeling was found to be a practical approach for this type of nonlinear system.

Nonlinear pseudo-modal models take a form analogous to a standard modal model except augmenting a single degree-of-freedom (DOF) system with a nonlinear forcing element. This element has taken many forms, from an Iwan element [6] to simple polynomial springs and dampers [5]. This approach relies on two primary assumptions. First, the modes of the system must remain uncoupled in the amplitude range of interest. Second, the mode shapes of the system must not change with amplitude. These assumptions allow for the use of a modal filter to obtain single degree-of-freedom signals in order to identify a nonlinear model. Like most nonlinear modeling techniques, the model is only accurate in the amplitude range used in parameter identification, so maximizing this amplitude range is of great interest.

In previous works [4, 7], the achievable structural response was not limited by mechanical factors but by the maximum allowable voltage output by the shaker amplifier. The objective of this work is to maximize the modal response using the windowed sinusoidal approach first presented in [4] by investigating the influnces of two factors of the input signal: frequency of the sine wave and the window width. An experimental bolted assembly was utilized in order to obtain linear and nonlinear response. Using a given shaker-amplifier configuration, the structure was tested with various windowed sinusoidal loadings to observe which properties of the input signal resulted in increased modal response amplitude, thus increasing the range for which the identified nonlinear model is valid.

This paper is organized as follows. Section 3 contains a brief description of the nonlinear pseudo-modal modeling technique, the modal filter, and a windowed sinusoidal excitation method. Section 4 shows the experimental system of interest and Section 5 details a standard nonlinear modal model fit to a baseline windowed sinusoidal excitation as performed in [4]. Section 6 shows the different experimental loading cases investigated and Section 7 compares the models obtained from select load cases. Finally, Section 8 contains conclusions from this study along with questions for future investigations.

3. Theory

This section provides an overview of the pseudo-modal model method used in this work to extract experimentally observed nonlinearity. The objective of this study is to compare the modal amplitude levels and models fit from different loading cases. Thus, this section also contains a summary of the modal filter and a detailed look at the arbitrary source excitation technique employed.

3.1 Nonlinear Pseudo-Modal Model

This work focuses on weakly nonlinear mechanical systems, which can be modeled as nonlinear pseudo-modal models. A nonlinear pseudo-modal model retains the assumptions of a linear modal model and acts similarly with a modal mass connected to ground by a spring and damper, but with the addition of an unknown nonlinear forcing element. Note that this technique assumes that the modes remain uncoupled and shapes do not change with amplitude. In [8], Eriten has shown a rigorous theoretical foundation for these assumptions in the presence of weak nonlinearities.

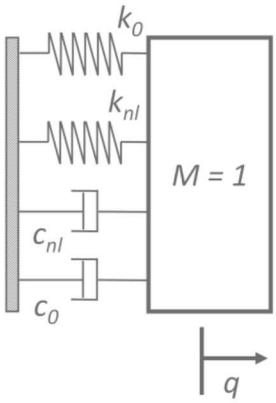

Fig. 1. Schematic of single degree-of-freedom nonlinear pseudo-modal model

For this work, the nonlinear forcing element are parameterized with polynomial springs and dampers as shown in Fig. 1. In order to identify these polynomial stiffness and damping coefficients a Restoring Force Surface [9] technique was implemented. A classical linear modal equation of motion is written as shown in Eqn. (1), where $\ddot{q}$, $\dot{q}$, and q are the modal acceleration, velocity, and displacement, c_0 and k_0 are the linear modal damping and stiffness, and $\phi^T F$ is the modal excitation force.

$$\ddot{q} + c_0\dot{q} + k_0 q = \phi^T F \tag{1}$$

The nonlinear elements are added to this equation of motion as seen in Eqns. (2) and (3). In Eqn. (2), F_{nl} is a generic nonlinear functional form, while in Eqn. (3) this is parameterized with quadradic and cubic springs and dampers, a form which has worked well in previous studies.

$$\ddot{q} + c_0\dot{q} + k_0 q \; + F_{nl} = \phi^T F \tag{2}$$

$$\ddot{q} + c_0\dot{q} + k_0 q \; + c_1\dot{q}|\dot{q}| + c_2\dot{q}^3 + k_1 q|q| + k_2 q^3 = \phi^T F \tag{3}$$

The mode shapes and linear coefficients (c_0 and k_0) are defined from low-level linear testing and the modal acceleration ($\ddot{q}$), velocity ($\dot{q}$), displacement (q), and force (F) are measured during a high-level test. Thus the procedure from [5] is implemented to obtain the nonlinear spring and damper coefficients c_1, c_2, k_1, and k_2. This procedure involves gathering terms with known or measured coefficients on one side of the equations and terms with unknown coefficients on the other as shown in Eqn.(4).

$$\overline{U} = \phi^T F - \ddot{q} - c_0\dot{q} - k_0 q \; = [\dot{q}|\dot{q}| \quad \dot{q}^3 \quad q|q| \quad q^3] \begin{bmatrix} c_1 \\ c_2 \\ k_1 \\ k_2 \end{bmatrix} = P \begin{bmatrix} c_1 \\ c_2 \\ k_1 \\ k_2 \end{bmatrix} \tag{4}$$

Note, the best parameters were obtained by transforming these quantities to the frequency domain, and stacking the real and imaginary parts of the signals as described in [5]. A least-squares estimate of these unknown coefficients are obtained by pre-multiplying $\overline{U}$ by the pseudo-inverse of experimental derived values P as in Eqn. (5). Using these polynomial coefficients, the nonlinear forcing element can now be used to predict the nonlinear response of this mode to several different loading cases.

$$\begin{bmatrix} c_1 \\ c_2 \\ k_1 \\ k_2 \end{bmatrix} = P^{+}\overline{U} \tag{5}$$

3.2 Modal Filter Theory

The nonlinear pseudo-modal model technique described in Section 3.1 relies on obtaining a single degree of freedom modal response. Thus, modal filtering is an essential step in the nonlinear modal modeling process. In this study, a spatial filter referred to here as the full-modal filter [10, 5] was used to isolate the single degree-of-freedom response for the target mode of the system.

In linear modal analysis, physical and modal accelerations are related through the linear mode shape matrix, $\boldsymbol{\Phi}$, as shown in Eqn. (6).

$$\boldsymbol{\Phi}\ddot{q} = \ddot{x} \tag{6}$$

By premultiplying the physical domain measurements with the Moore-Penrose pseudo-inverse of the mode shape matrix, measured modal responses can be obtained (see Eqn. (7)). This filtering is key to the nonlinear pseudo-modal modeling process and thus sufficient instrumentation must be used in order to properly filter the modes.

$$\ddot{q} = \boldsymbol{\Phi}^{+}\ddot{x} \tag{7}$$

3.3 Experimental Applied Force

Hammer and shaker excitation techniques were studied and compared in [4]. For this study, the windowed sinusoid approach discussed in [4] was used to excite an experimental structure to high excitation levels. This has been found to be a practical way to obtain high amplitude response of a single mode. The windowed sinusoid approach takes a sine wave at a designated center frequency, f_e, and applies a window to modulate the amplitude. This signal is used as the input voltage to the amplifier that powers the modal shaker. Because of the window, the frequency content of the signal is not contained solely at f_e, but spread over the frequency band $f_e \pm \Delta f_r$, where Δf_r is the excitation bandwidth determined by the window function. . Figure 2 shows this input voltage in the frequency domain, while Figure 3 shows the input voltage, sine wave, and window in the time domain.

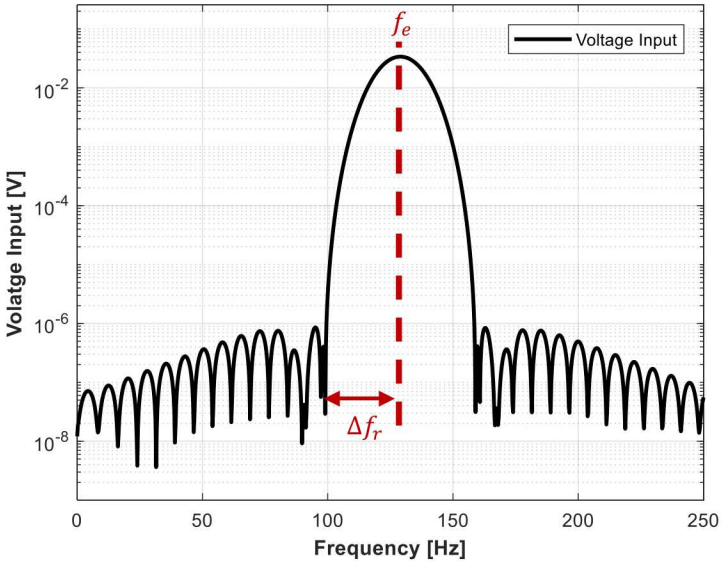

Fig. 2. Arbitrary voltage input for a windowed sinusoidal excitation

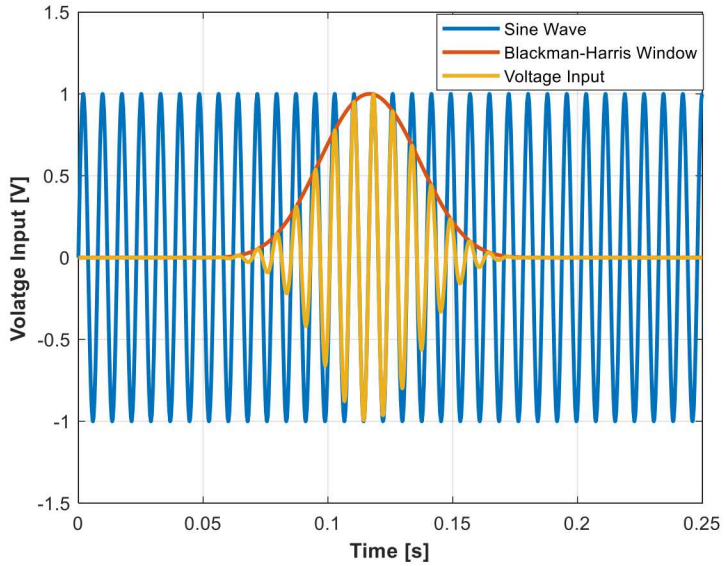

Fig. 3. Example windowed sinusoidal input

Spreading of the frequency content is ideal for nonlinear investigations. Often, a weakly nonlinear system contains a small shift in resonant frequency as amplitude is increased. Therefore, a single tone sine wave may not input sufficient energy into a nonlinear mode as the system softens or hardens unless the frequency is constantly updated to match the shifting resonance.

The windowed sinusoid spreads the frequency content to help ensure the system has some excitation energy at resonance regardless of shifting due to nonlinearity. In past studies, windows with large Δf_r were used to ensure energy was input at resonance. Signals with large Δf_r in the frequency domain correspond to short pulses in the time domain, which reduces the excitation of the target mode. During testing, amplifier voltage limits were typically reached, reducing the achievable response amplitude of the mode. It was theorized that concentrating the input energy over a narrower band and shifting it near where the nonlinear resonance of the mode is expected to transition to at

higher response levels would result in larger responses without exceeding the electrical limits of the amplifier. For example, if preliminary tests show that the target mode is softens at high amplitude, then f_e is set to be lower than the linear natural frequency. However, if the band is too narrow, the mode may soften or harden past the input energy band and fall off-resonance, therefore, a balance must be achieved such that a high response level is achieved while also continuously excitingthe mode's resonance. This study iterates on the center frequency, f_e, and excitation bandwidth, Δf_r, in order to optimize the response of a target mode of a jointed structure. Note that in previous works [4, 7], a triangle window was used on the sinusoid, but in more recent works and this study, a Blackman-Harris [11] window was utilized. The latter is preferred as it has lower side lobes in the frequency domain which allows for more energy input in the frequency band of interest.

4. Experimental Set-Up

4.1 Hardware Description

A picture of the experimental set-up is shown in Fig. 4. The hardware consists of an aluminum beam and plate connected with two bolts and a layer of epoxy. This subassembly is connected to an aluminum cylinder with eight bolted joints along a large continuous interface. This system is referred to as the Cylinder-Plate-Beam (CPB) and has been the focus of many nonlinear studies including [5, 4, 7].

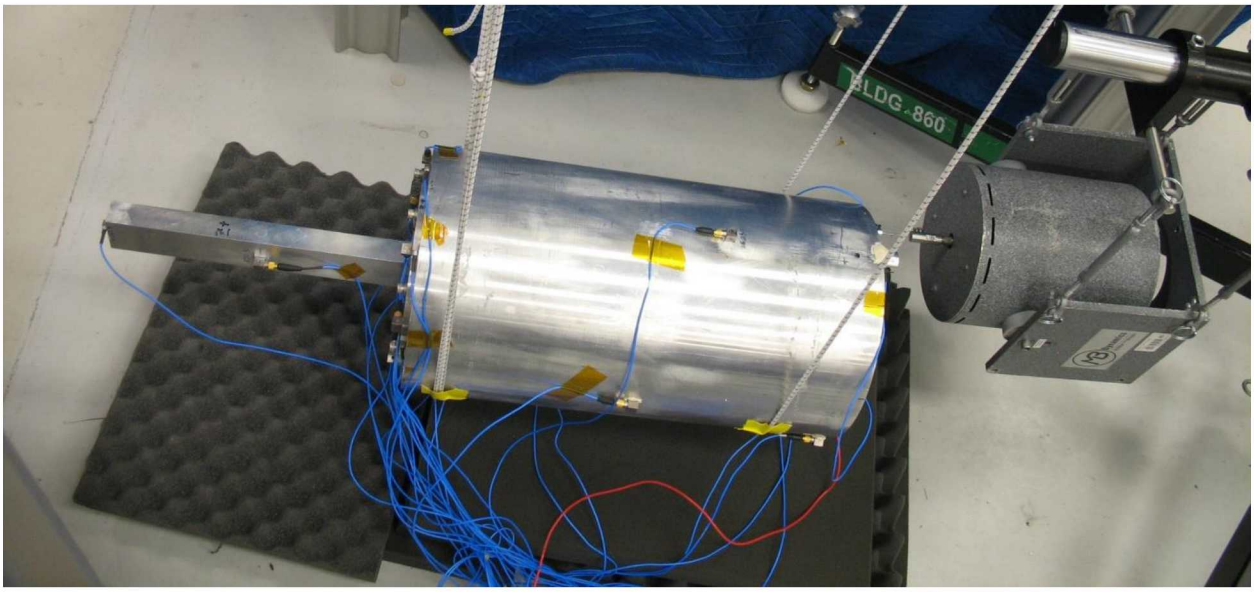

Fig. 4. Physical CPB hardware configuration

The system was instrumented with 26 triaxial accelerometers in the same configuration as tested in [4]. These were selected using mode shapes from a finite element model to ensure independent shapes below 1,600 Hz. The CPB was suspended using two bungee cords to approximate a free-free boundary condition. For all testing, a force transducer and shaker set-up were attached at the rear of the cylinder. This shaker was used to perform low-level burst random testing as well as high-level arbitrary source excitations.

4.2 Linear Model Extraction

A low-level burst random test was performed in order to obtain linear modal parameters. The linear shapes from this test were used to filter high-level accelerometer measurements into single degree-of-freedom modal responses while the linear natural frequencies and damping ratios were used as known quantities during the nonlinear identification process. The linear natural frequencies and damping ratios of the system are shown in Table 1.

Table 1 – Linear modal parameters

Mode	f_n [Hz]	ζ [% cr]	Shape Description

7	129.6	0.397 %	1st soft bending of Beam
8	172.6	0.322 %	1st stiff bending of Beam
9	385.8	0.069 %	(2,0) Ovaling model
10	391.9	0.083 %	(2,0) Ovaling model
11	551.6	0.278 %	Axial mode
12	945.4	0.413 %	(3,0) Ovaling model
13	1025.7	0.076 %	2nd soft bending of Beam

5. Nonlinear Modal Model Extraction Overview

In this section, the results from a traditional windowed sinusoid excitation are analyzed resulting in a nonlinear pseudo-modal model.

The procedure used to identify nonlinear pseudo-modal models from experimental data as described in Section 3.1 can be broken into three main steps. First, a high-level excitation must be applied, such as the windowed sinusoid discussed in Section 3.3. Next, a single degree-of-freedom modal response must be obtained, often with the use of a spatial modal filter. Finally, using this modal response the restoring force surface technique described in Section 3.1 can be used to identify a nonlinear pseudo-modal model that best fits the measured data in a least squares sense.

Fig. 5. Model process overview

For a baseline, the CPB was tested using a wide-bandwidth windowed sinusoid. For this initial test, the structure was excited using a windowed sinusoid where the center frequency, f_e, was the first linear natural frequency of 130 Hz, and the excitation bandwidth, Δf_r, was $\pm$ 30 Hz. This provides a wide pulse of energy in the frequency domain near the first bending resonance of the structure. The voltage level was tuned to maximize the voltage output of the amplifier without exceeding the electrical limits. After applying the modal filter, the accelerometer measurements were transformed into a single DOF response of the first bending mode. Figure 6 shows the applied modal force and response in the time domain, while Fig. 7 shows the data in the frequency domain.

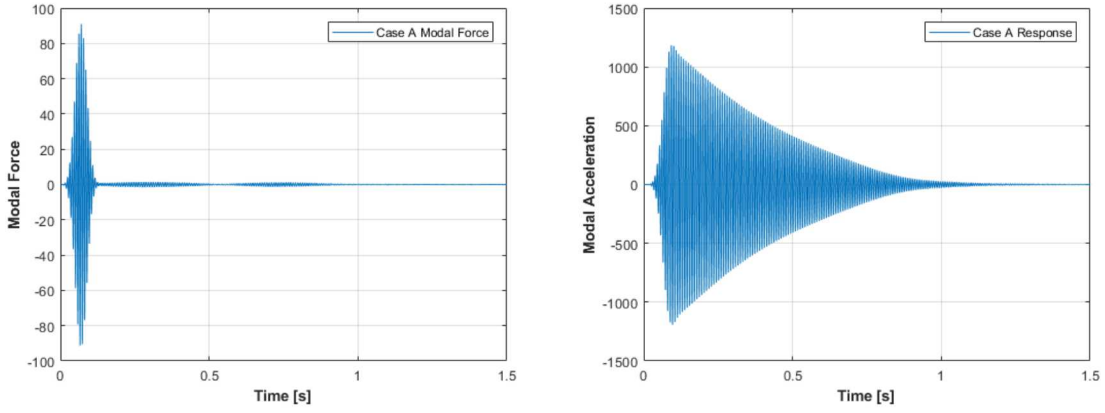

Fig. 6. Time domain modal force and acceleration

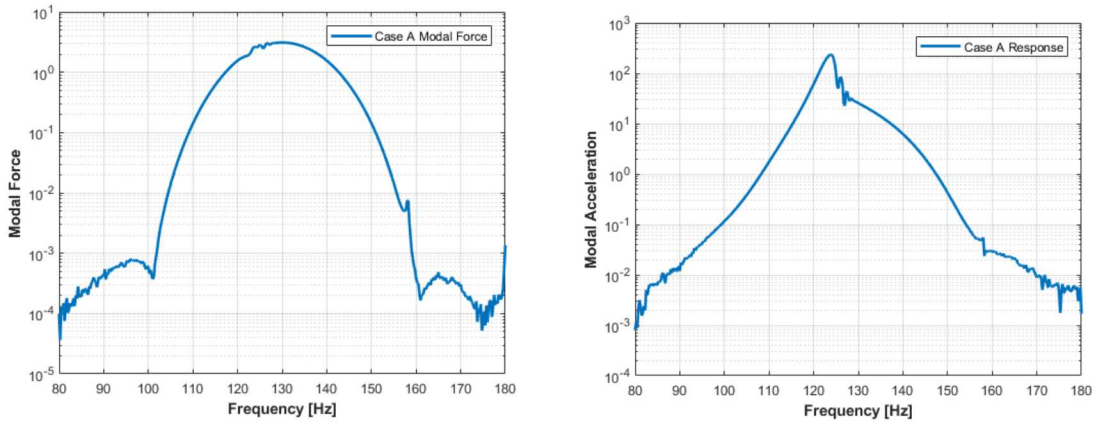

Fig. 7. Frequency domain modal force and response

Following the RFS procedure from Section 3.1, a nonlinear modal model was extracted using a cubic and quadradic polynomial spring and damper as the nonlinear forcing elements. A simulation of the model was performed and obtained good agreement with the measured response data as shown in Fig. 8. Early in time, at high amplitude levels, the signals have great correlation, while later in time the measurement has more damping and the model begins to overpredict. This wide bandwidth windowed sinusoid is similar to those applied to the system in recent works [4], where results with similar accuracy were obtained. The slight degredation in the prediction late in time is believed to be a result of the least-squares fitting since this method biases the coefficients to minimize the error at the high amplitude responses.

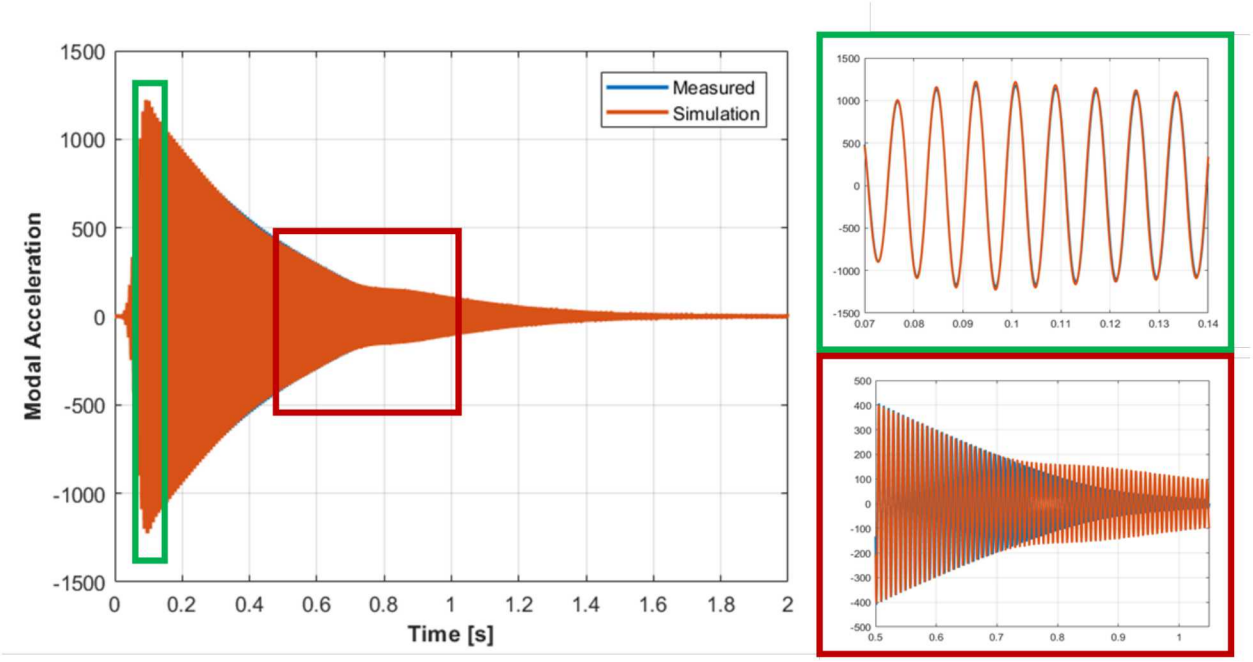

Fig. 8. Simulated response for baseline case

6. Experimental Results to Modified Windowed Sinusoidal Inputs

In order to optimize modal amplitude, the values of f_e and Δf_r were adjusted from this baseline case to observe the impact of these input parameters on the modal amplitude achieved for the mode of interest. These test cases are summarized in Tables 2, 3, and 4. First, the center frequency was held constant and the excitation bandwidth, Δf_r, was narrowed from 30 Hz to 20, 10 and 5 Hz respectively. By narrowing Δf_r but maintaining the same maximum voltage,

the applied force provided additional margin to the shakers electrical limits, allowing the applied force to be increased. These are represented in Test Cases A-D.

Next the system was excited with a windowed sinusoid with a shifted center frequency. Note that the testing was conducted over a period of two days, during which the linear natural frequency of the target mode shifted. Thus, a new baseline case is contained in Test Case E, and Test Cases F-H contain correspond to experiments with shifted center frequencies. From preliminary testing and previous studies conducted on this structure, the target mode is known to soften, so Cases F-H have center frequencies lower than the linear natural frequency. Case F retained the baseline 30 Hz window width. Case G applied a force with a center frequency of 119 Hz but narrows the excitation bandwidth to ±5 Hz. Finally, Case H lowers the input voltage of Case G to obtain approximately the same modal amplitude as the second baseline case.

6.1 Experimental Results from Cases A-D

Table The results of Experimental Cases A-D are shown in Figures 9 and 10, where Figure 10 shows the modal response obtained from the excitation inputs displayed in Figure 9. The frequency band from ±30 Hz to ±5 Hz to see the effect on the resulting modal amplitude. The windowed sinusoid signal parameters are summarized in Table 2.

Table 2 – Windowed sinusoidal signal parameters Cases A-D

Test Case	f_e [Hz]	Δf_r [Hz]	Amplifier Level	Description
A	130	±30	70	Baseline
B	130	±20	70	-
C	130	±10	70	-
D	130	±5	70	-

As shown in Figure 10, the broadband frequency input of Case A does apply a smaller force in the frequency domain than the narrower window Cases B-D. In a linear system, the higher modal forces would be expected to obtain higher modal response but the opposite is seen in Case D where the forcing is concentrated in a narrow band around the linear natural frequency. Recall the nonlinearity for this mode results in a softening effect. The lower modal amplitude at a higher force implies that, as the mode achieved higher response levels, its resonant frequency decreased out of the excitation bandwidth. Conversely, loading from Case B provided the highest modal response without applying the highest modal force, so there is an optimal excitation bandwidth for exciting a high modal response.

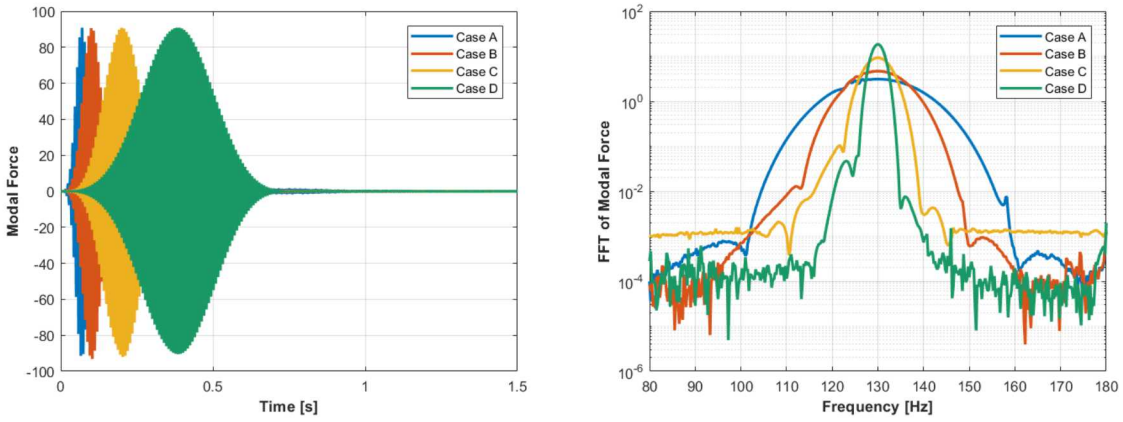

Fig. 9. Cases A-D modal response time and frequency response

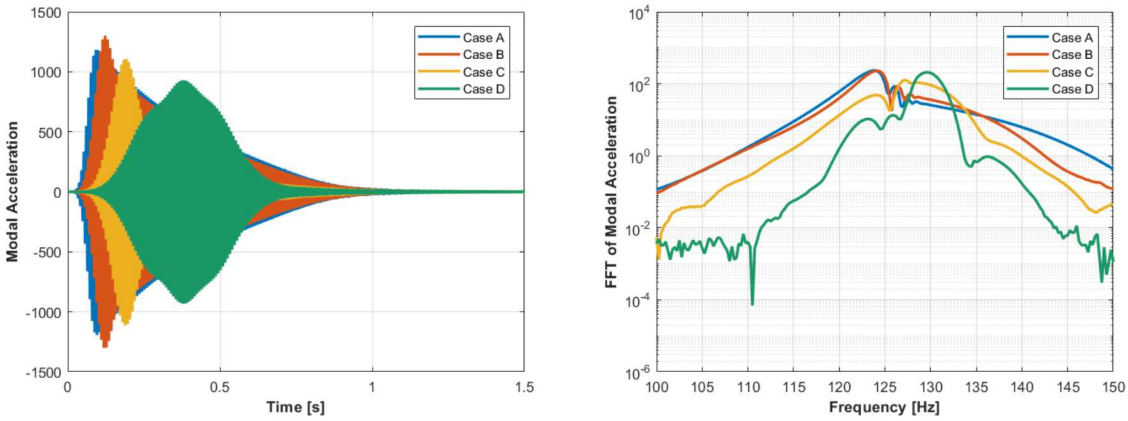

Fig. 10. Cases A-D acceleration time and frequency response

The instantaneous frequency of each of the above cases was computed as the inverse of the oscillation period as determined from the zero crossings in the respective responses, see Figure 11. The initial timeframes, t_i, begin near 130 Hz which was the selected forcing frequency for these experiments. As the amplitude increases, each of the experimental cases follows a different trajectory as the frequency traces through the response transient. Eventually, Cases A-C converge onto the same curve and end at the final time, t_f. Note that as the signals become smaller, the calculated instantaneous frequency becomes very noisy, so only a certain amplitude range of data was considered which is why the curves do not end at the linear natural frequency of 130 Hz. Cases A and B lay on the same curve as the frequency shifts from ~122 Hz back to ~128 Hz. Case D never falls onto this curve because the by the time the force response ends the signal is almost fully decayed. This is confirmed in the time histories shown in Figure 9 and 10. These case studies show that an optimal window width can be selected to maximize modal amplitude but a balance must be achieved such that the excitation envelopes the shift in the nonlinear resonance Ideally, a quality nonlinear pseudo-modal model would match all time responses as it should be able to accommodate complicated, potentially off-resonance loadings.

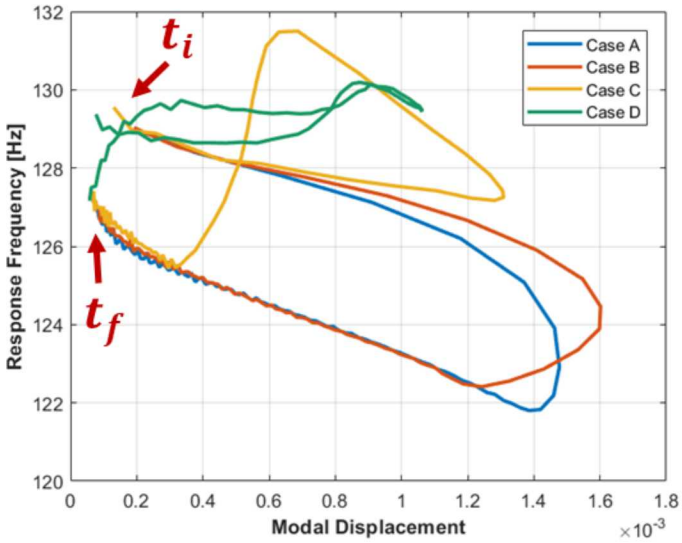

Fig. 11. Cases A-D frequency tracking

6.2 Experimental Results from Cases E-F

With the insight gained from Cases A-D, another series of tests were conducted with the center frequency of the windowed sinusoid shifted from the linear natural frequency of the target mode. This was accomplished by adjusting f_e in the input voltage signal. These new loading signals, Cases E-G, are summarized in Table 3.

Table 3 – Windowed sinusoidal signal parameters Cases E-G

Test Case	f_e [Hz]	Δf_r [Hz]	Amplifier Level	Description
E	129	±30	70	Second Baseline
F	119	±30	70	-
G	119	±5	70	-

This shifted resonance study consists of Case E-G shown in Figures 12 and 13. Cases E and F provide nearly identical results, with both reaching around the same modal amplitude while Case G magnifies the modal amplitude by over a factor of 2 in the time domain. With more optimization on center frequency shift and excitation bandwidth, this magnification could be even higher. The modal response also has a second pulse as can be observed in Figure 13.

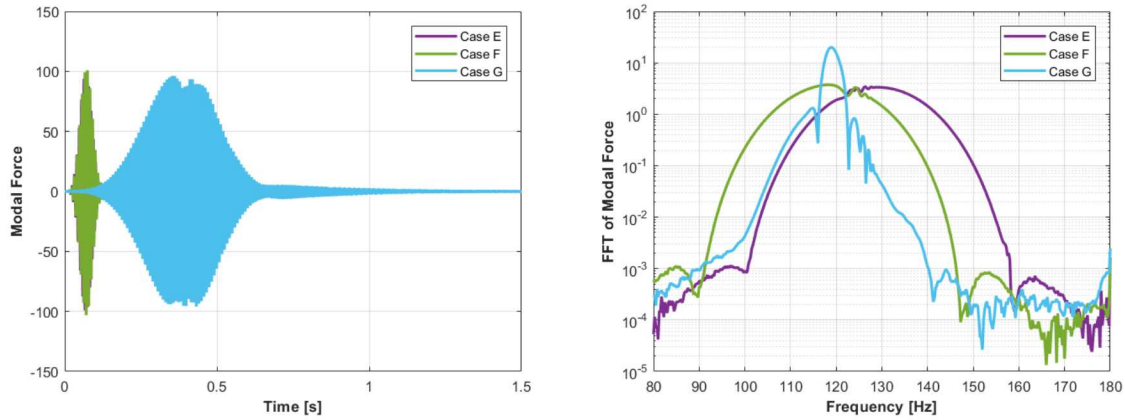

Fig. 12. Cases E-G modal response time and frequency response

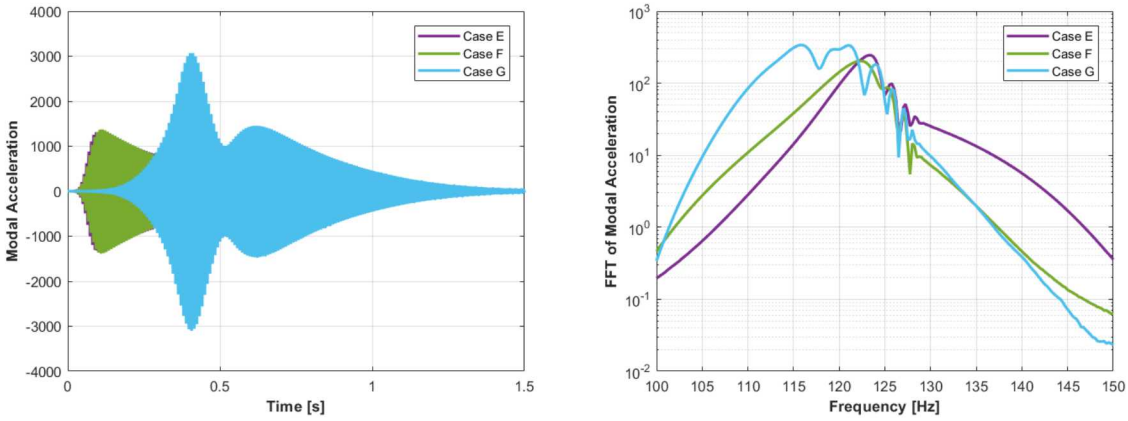

Fig. 13. Cases E-G modal acceleration time and frequency response

Figure 14 shows the frequency tracking plot for Cases E-G. Here, the responses of Case E and F begin near their respective forcing frequencies. Both cases eventually converge to the same backbone during the free decay portion of the transient. Case G begins at the forced natural frequency of around 119 Hz, then softens as it reaches peak modal

amplitude down to around 114 Hz before hardening to around 125 Hz. The signal of the response, while under forced response conditions, appears to be semi-bounded by the excitation bandwidth Δf_r set of ±5 Hz.

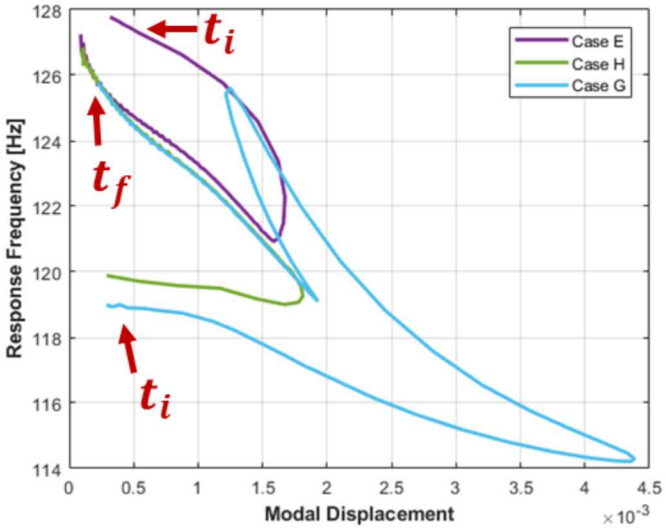

Fig. 14. Cases E-G frequency tracking

6.3 Experimental Results from Cases E and H

In order to evaluate the nonlinear models extracted from varying inputs, the voltage input from Case G was scaled until it excited the same modal amplitude as Case E. The second baseline and the new loading signal, Case H, are shown in Table 4.

Table 4 – Windowed sinusoidal signal parameters Cases E and H

Test Case	f_e [Hz]	Δf_r [Hz]	Amplifier Level	Description
E	129	±30	70	Second Baseline
H	119	±5	43	Matched Amplitude

This new loading case is shown as Case H in Figures 15-17. While the modal amplitudes are similar, the peak modal force required for Case H is much smaller. Figure 17 shows the frequency tracking for these two cases which behave as expected: the initial frequency of each response is near their corresponding forcing frequencies and then the free-decay portions overlay near the end of the transient. In the next section, models fit from these two cases are compared in order to understand how shifting f_e influences the model obtained from a restoring force surface identification process.

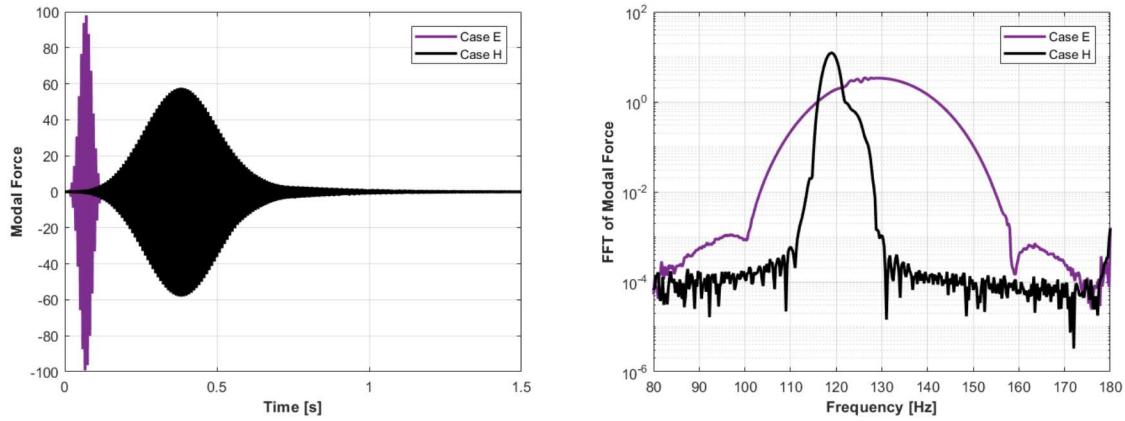

Fig. 15. Cases E and H modal force time and frequency response

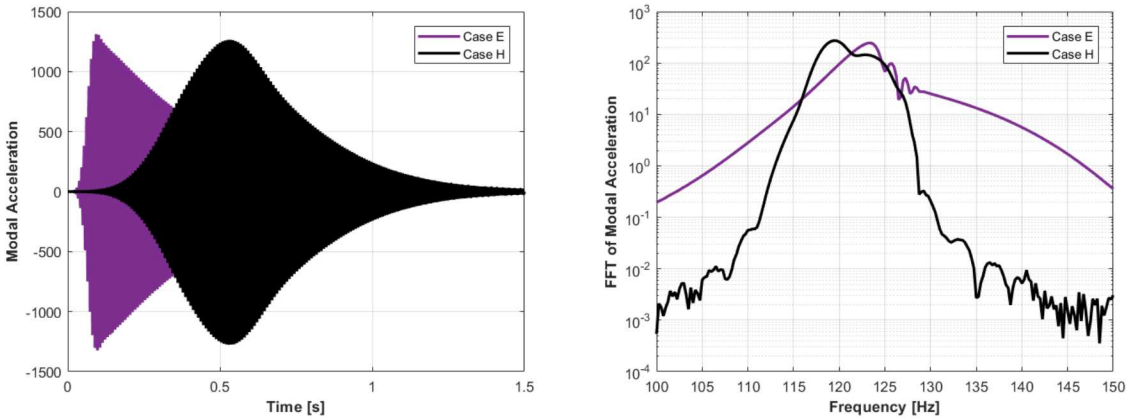

Fig. 16. Cases E and H modal acceleration time and frequency response

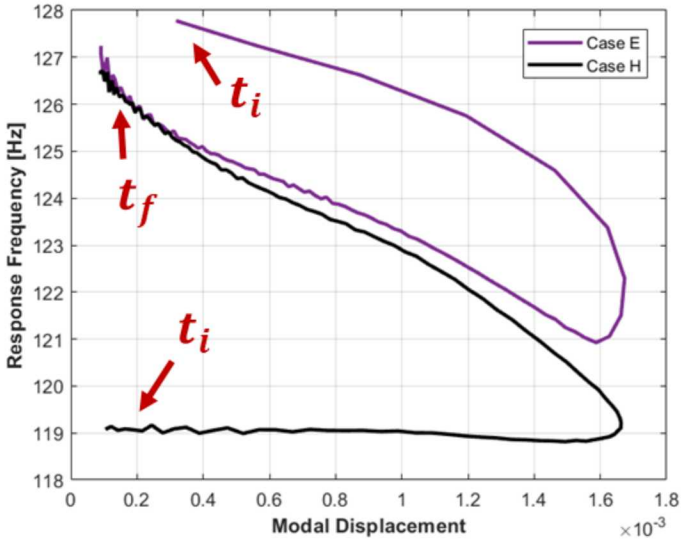

Fig. 17. Cases E and H frequency tracking

7. Model Comparison

The restoring force surface technique outlined in Section 3.1 was implemented in order to find nonlinear modal models for Cases E, G and H. For convienance, the loading parameters for these simulations, Cases E, G and H, are shown in Table 5.

Table 5 – Windowed sinusoidal signal parameters Cases E, G, and H

Test Case	f_e [Hz]	Δf_r [Hz]	Amplifier Level	Description
E	129	±30	70	Second Baseline
G	119	±5	70	-
H	119	±5	43	Matched Amplitude

The cubic and quadradic polynomial stiffness and damping coefficients obtained are displayed in Table **Error! Reference source not found.**. Note, the value of these coefficients are drastically different for Cases E and G. This is expected as these two tests reached different modal amplitude levels and used the same model order to fit this different range of amplitudes. Comparing the coefficients from Cases E and H is more useful as these two cases reached nearly the same modal amplitude level but used different values of f_e and Δf_r. The models obtained for these two cases are nearly identical showing that peak modal amplitude is more influential in the model than the center frequency and/or window width.

Table 6 – Nonlinear coefficients for cases E, G and H

Test Case	Case E	Case G	$\%_{diff,EG}$	Case H	$\%_{diff,EH}$
k_1	-7.50E+07	-5.63E+07	-25%	-7.28E+07	-3%
k_2	1.54E+10	4.73E+09	-69%	1.37E+10	-11%
c_1	-1.489	-1.186	-20%	-1.403	-6%
c_2	-0.025	0.109	-536%	-0.034	36%

The response of the target mode was simulated using two different models: one identified from the Case E measurements and the other from Case G measurements. The forcing for both of these simulations is that from Case E. The results are shown in Figure 18. Both simulations compare to measured data favorably with the Case E model performing slightly better, as it overlays with the measured in late time. The error in the late time simulation using the Case G model is similar to the error seen in previous studies [4]. Even with different coefficient values for the nonlinear models, the two models exhibited similar nonlinear effects in the response range achieved with Case E forcing. Figure 19 displays the effective stiffness and damping for each of these models where $k_{eff} = k_0 + k_1|q| + k_2 q^2$ and $c_{eff} = c_0 + c_1|\dot{q}| + c_2 \dot{q}^2$. These show good agreement between the two models but the Case G model goes to a higher modal amplitude. There is a slight discrepancy in modal effective dissipation, potentially due to the nature of the forced response of Case G model but this is a topic for future study.

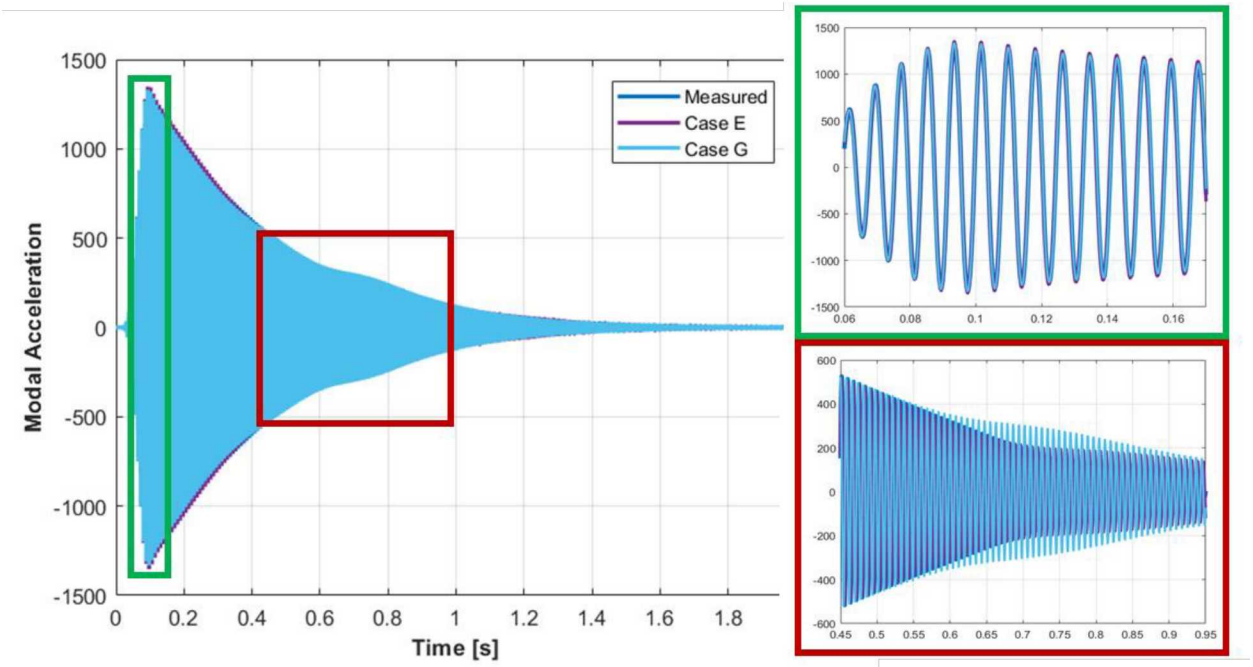

Fig. 18. Cases E and G simulations to Case E forcing

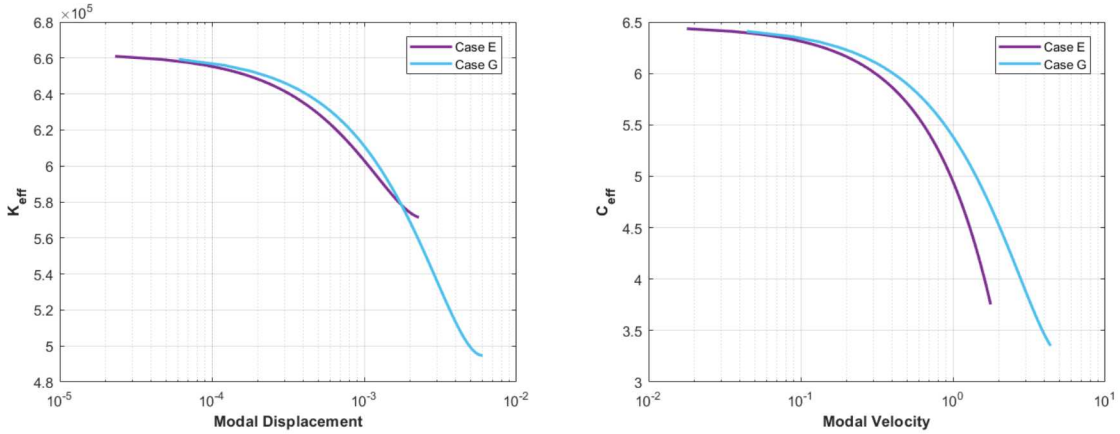

Fig. 19. Effective stiffness and damping for Cases E and G

Next, the Case G loading was applied to the same two models. Here, the Case G model vastly outperforms the Case E system. This is expected as the Case E simulation has to extrapolate to reach the modal response levels of the Case G excitation.

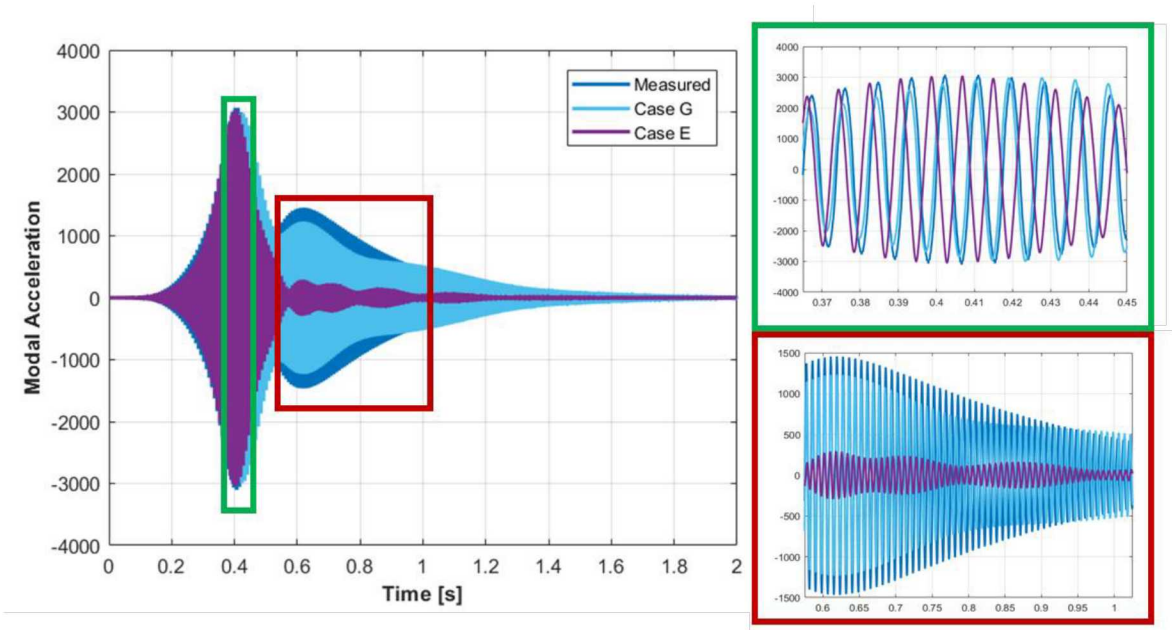

Fig. 20. Cases E and G simulation to Case G

Finally, models identified from Case E and Case H were used to simulate the response of the target mode to the Case H loading, see Figure 21. The results of the two simulations are very similar which is to be expected given that they had very little difference in their nonlinear coefficient values. so they are expected the perform similarly. As shown in Figure 21, the Case E model can capture the milder second pulsing of this loading case and the effective stiffness and damping curves overlay as shown in Figure 22. Neither model matches the measured response for the entire transient like the baseline loading presented in Section 5 and this should be a topic for further study.

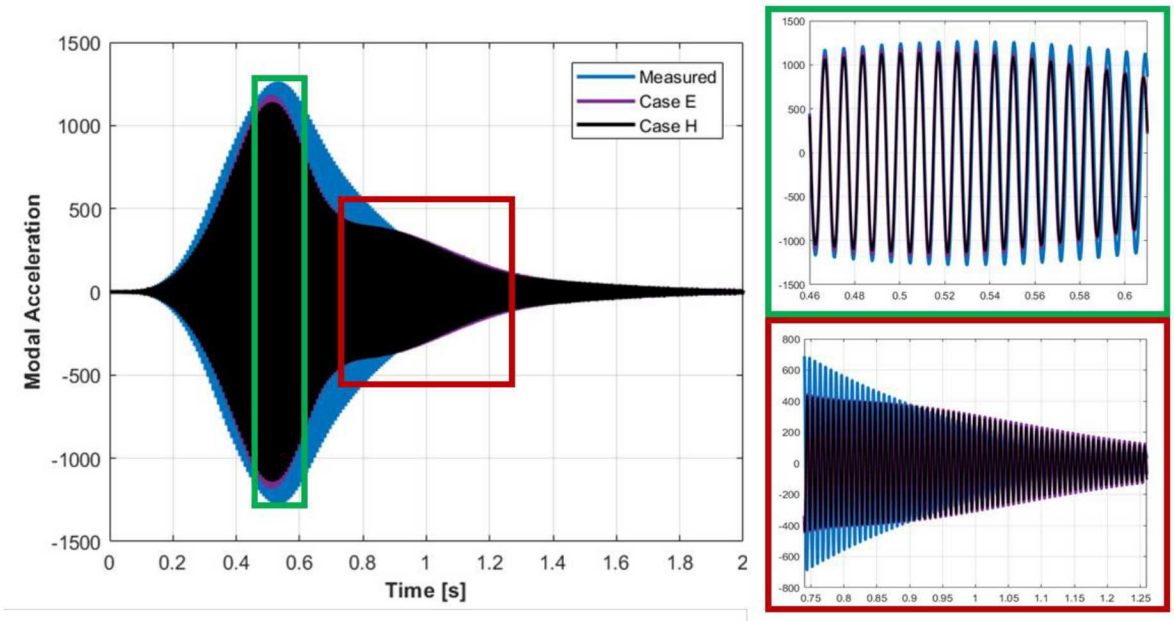

Fig. 21. Cases E and H simulation to Case H

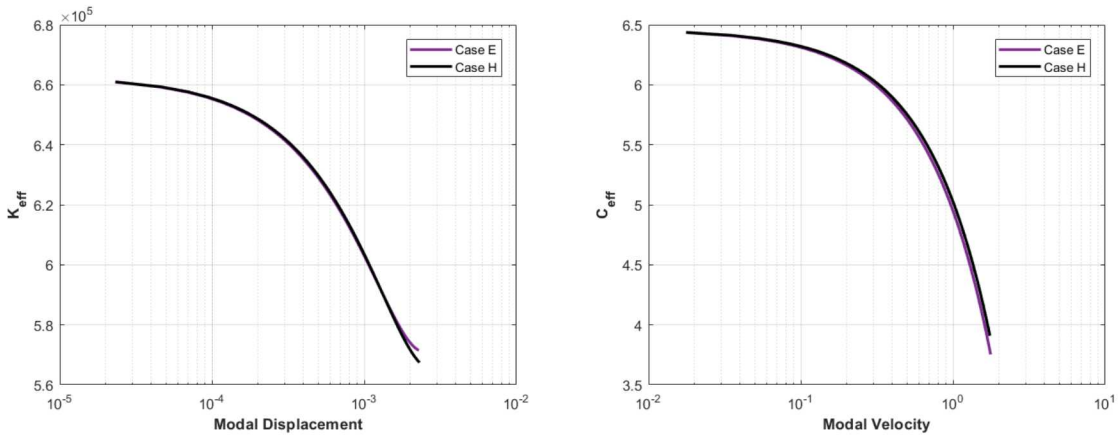

Fig. 22. Effective stiffness and damping for Cases E and H

8 Conclusions and Future Work

Nonlinear models identified from experiments are only accurate to the response amplitudes achieved during testing, thus obtaining higher modal amplitudes during experiments is very important to the versatility of the identified models. This work demonstrated new innovative techniques for optimizing modal amplitude given a specific shaker and amplifier configuration. These techniques were implemented on a bolted assembly consisting of an aluminum cylinder, plate, and beam. In previous studies, windowed sinusoidal inputs proved to be a useful excitation technique when attempting to reach high modal amplitudes in a jointed structure. In previous studies, this sinusoidal pulse was centered around the linear natural frequency. In this work, the windowed sinusoidal technique was implemented with varied window widths and center frequencies with the goal of placing more energy near the expected resonance of the structure which softened due to nonlinearity. By applying a narrow window at an offset frequency, the modal amplitude achieved double that of previous tests using the same set-up. Additional optimization could be performed to increase the amplification to even higher levels and is of interest for future work. This amplification is significant as it means natural excitations slightly off of linear resonance can still lead to large response due to a nonlinearity in the structure.

A restoring force surface technique was applied to identify several nonlinear models from experiments with different load cases to capture the nonlinearity of the structure for the mode of interest. It was shown that the model identified from a standard windowed sinusoidal excitation was equivalent to that of the new technique, provided, they both excite the system to the same modal amplitude. Additionally, a model identified from a data set with even higher modal amplitude provided a quality fit for the standard excitation providing a model more versatile of multiple excitation configurations.

References

[1] D. Segalman, "A Modal Approach to Modeling Spatially Distributed Vibration Energy Dissipation," Sandia National Labs SAND2010-4763, Albuquerque, NM, 2010.

[2] B. J. Deaner, Modeling the Nonlinear Damping of Jointed Structures Using Modal Models, Masters of Science Thesis: University of Wisconsin, Madison, 2013.

[3] D. Roettgen and M. Allen, "Nonlinear characterization of a bolted, industrial structure using a modal framework," *Mechanical Systems and Signal Processing,* vol. 84, 2016.

[4] B. R. Pacini, R. L. Mayes, B. C. Owens and R. Schultz, "Nonlinear Finite Element Model Updating, Part I: Experimental Techniques and Nonlinear Modal Model Parameter Extraction," in *International Modal Analysis Conference XXXV*, Garden Grove, CA, 2017.

[5] R. L. Mayes, B. R. Pacini and D. R. Roettgen, "A Modal Model to Simulate Typical Structural Dynamic Nonlinearity," in *International Modal Analysis Conference XXXIV*, Orlando, FL, 2016.

[6] D. J. Segalman, "A Four-Parameter Iwan Model for Lap-Type Joints," *Journal of Applied Mechanics,* vol. 72, pp. 752-760, 2005.

[7] D. Roettgen, B. Pacini, R. Mayes and T. Schoenherr, "Experimental-Analytical Substructuring of a Complicated Jointed Structure Using Nonlinear Modal Models," in *International Modal Analysis Conference XXXVI*, Orlando, FL, 2018.

[8] M. Eriten, M. Kurt, G. Luo and A. Vakakis, "Nonlinear system idenfitication of frictional effects in a beam with a bolted joint connection," *Mechanical Systems and Signal Processing,* vol. 39, pp. 245-264`, 2013.

[9] G. Kerschen, K. Worden, A. Vakakis and G. J-C., "Past, present and future of nonlinear system identification in structural dynamics," *Mechanical Systems and Signal Processing,* vol. 20, no. 3, pp. 505-592, 2006.

[10] S. Spottswood and R. Allemang, "On the Investigation of Some Parameter Identification and Experimental Modal Filtering Issues for Nonlinear Reduced Order Models," *Experimental Mechanics,* vol. 47, pp. 511-521, 2007.

[11] F. Harris, "On the use of windows for hamonic analysis with the discrete fourier transform," in *Proceedings of the IEEE*, 1978.

[12] D. P. Hensley and R. L. Mayes, "Extending SMAC to Multiple References," in *International Modal Analysis Conference XXIV*, 2006.